
SHARPNESS OF MINIMA IN DEEP MATRIX FACTORIZATION: EXACT EXPRESSIONS

Anil Kamber, Rahul Parhi

Department of Electrical and Computer Engineering
University of California, San Diego
{akamber, rahul}@ucsd.edu

ABSTRACT

Understanding the geometry of the loss landscape near a minimum is key to explaining the implicit bias of gradient-based methods in non-convex optimization problems such as deep neural network training and deep matrix factorization. A central quantity to characterize this geometry is the maximum eigenvalue of the Hessian of the loss, which measures the sharpness of the landscape. Currently, its precise role has been obfuscated because no exact expressions for this sharpness measure were known in general settings. In this paper, we present the first exact expression for the maximum eigenvalue of the Hessian of the squared-error loss at any minimizer in general overparameterized deep matrix factorization (i.e., deep linear neural network training) problems, resolving an open question posed by Mulayoff & Michaeli (2020). To complement our theory, we empirically investigate an escape phenomenon observed during gradient-based training near a minimum that crucially relies on our exact expression of the sharpness.

1 INTRODUCTION

Decades of research in learning theory suggest limiting model complexity to prevent overfitting. However, modern deep learning is heavily overparameterized and has nonetheless achieved unprecedented success in practice over the past decade (Krizhevsky et al., 2012; Vaswani et al., 2017). Generally, in overparameterized settings, the loss function has infinitely many global minima that achieve zero training error (interpolation regime), yet these models still perform well. This phenomenon has been explored in various settings such as nonparametric regression, (Belkin et al., 2019), training two-layer neural networks with logistic loss (Frei et al., 2022), and linear regression (Bartlett et al., 2020).

The propensity of neural network training dynamics to converge to *good minima* is attributed to the ability of gradient-based optimization algorithms to avoid *bad minima* (Neyshabur et al., 2017; Zhang et al., 2017). This is related to the *implicit bias* of gradient descent (GD) (Neyshabur et al., 2014), and a large body of work has focused on its understanding (Gunasekar et al., 2017; 2018; Soudry et al., 2018; Arora et al., 2019; Ji & Telgarsky, 2020; Yun et al., 2021).

It has been observed that *dynamical stability* of GD near a minimum is a key factor in characterizing its implicit bias toward particular solutions (Wu et al., 2018; Nar & Sastry, 2018). Conceptually, dynamical stability refers to the ability of GD to *stably converge* to a minimum, and it is closely related to the sharpness of the loss landscape in its vicinity (Mulayoff et al., 2021). This topic has been investigated in numerous works (Nar & Sastry, 2018; Wu et al., 2018; Ma & Ying, 2021; Mulayoff et al., 2021; Nacson et al., 2023; Qiao et al., 2024; Liang et al., 2025) within the framework of the classical notion of *linear stability* in dynamical systems (Strogatz, 2024).

Ultimately, this understanding boils down to understanding the *geometry* of the loss landscape near a minimum. The maximum eigenvalue of the Hessian of the loss serves as a key measure to quantify the *sharpness* of the landscape near a minimum. Despite its significance, its precise role is not well-understood, particularly because closed-form expressions are generally unknown, outside a few particular cases. We summarize current state of understanding as well as the contributions of our paper in Table 1.

Table 1: Closed-form expressions for the maximum Hessian eigenvalue in the literature. Ω denotes the set of *all* global minimizers, $\Omega_0 \subseteq \Omega$ denotes the set of *flat* global minimizers, and $\Omega_B \subseteq \Omega$ denotes the set of *balanced* global minimizers.

Related Work	Depth	Input Dim.	Output Dim.	$\lambda_{max}(\nabla^2 \mathcal{L}(\mathbf{w}))$	Layers
(Mulayoff & Michaeli, 2020)	L	d_0	d_L	$\mathbf{w} \in \Omega_0$	$\mathbb{R}^{a \times b}$
(Zhu et al., 2023)	2	1	1	$\mathbf{w} \in \mathbb{R}^N$	\mathbb{R}
(Singh & Hofmann, 2024)	2	1	1	$\mathbf{w} \in \mathbb{R}^N$	\mathbb{R}^a
(Ghosh et al., 2025)	L	d_0	d_L	$\mathbf{w} \in \Omega_B$	$\mathbb{R}^{a \times b}$
Theorem 5 (This Paper)	L	d_0	d_L	$\mathbf{w} \in \Omega$	$\mathbb{R}^{a \times b}$

Most notably, the seminal work of Mulayoff & Michaeli (2020) derives a closed-form expression for the maximum eigenvalue of the Hessian at *flat* global minima of deep linear networks (i.e., deep matrix factorization) with squared-error loss. However, obtaining a closed-form expression for *all* global minima in deep linear networks/deep matrix factorization was an open problem. In particular, Mulayoff & Michaeli (2020) claim that finding a closed-form expression for arbitrary global minima is intractable. In this paper, we refute this claim and positively answer the following fundamental question.

Does a closed-form expression for the maximum eigenvalue of the Hessian exist for overparameterized deep matrix factorization problems?

In particular, in Theorem 5, we provide a closed-form expression for the maximum Hessian eigenvalue at arbitrary minima of depth- L overparameterized deep matrix factorization. To the best of our knowledge, our analysis provides the first exact expression of the maximum eigenvalue for deep matrix factorization/deep linear neural network problems. In the case of deep overparameterized scalar factorization (Theorem 4) and depth-2 matrix factorization (Corollary 6), our closed-form expression simplifies considerably.

With our closed-form expression in hand, we then empirically explore in Section 5 the *escape phenomenon*, observed by Wu et al. (2018) (who only studied a one-dimensional setting). We find that this phenomenon also occurs for overparameterized deep matrix factorization problems. Therefore, we empirically observe the following.

GD always escapes from a dynamically unstable minimum, regardless of how close the initialization is to that minimum.

We explore this phenomenon through the lens of *dynamical stability* and, in particular, the notion of *dynamically unstable* minima introduced by Nar & Sastry (2018) and Wu et al. (2018). Their definition is as follows.

Definition 1 (see Wu et al. 2018, Definition 1). *Let \mathbf{x}^* be a minimum of a loss function \mathcal{L} . Consider the linearized GD dynamics about \mathbf{x}^**

$$\mathbf{x}_{t+1} = \mathbf{x}_t - \eta \nabla^2 \mathcal{L}(\mathbf{x}^*)(\mathbf{x}_t - \mathbf{x}^*), \quad (1)$$

where η is the step size and $\nabla^2 \mathcal{L}(\mathbf{x}^*)$ is the Hessian matrix of the loss function at \mathbf{x}^* . Then, \mathbf{x}^* is said to be dynamically unstable if, for every constant $C > 0$, there exists a $t > 0$ such that

$$\|\mathbf{x}_t\|_2^2 > C \|\mathbf{x}_0\|_2^2. \quad (2)$$

We rely on the necessary and sufficient conditions established by Wu et al. (2018) for a minima \mathbf{x}^* to be dynamically unstable. Their condition is that $\lambda_{\max}(\nabla^2 \mathcal{L}(\mathbf{x}^*)) > 2/\eta$. Thus, we see that an exact expression for the maximum eigenvalue is necessary to sharply explore the escape phenomenon.

1.1 RELATED WORK

Flat Minima. Mulayoff & Michaeli (2020) derived a closed-form expression for the maximum eigenvalue of the Hessian at flat minima for deep linear neural networks. They also showed that the Hessian at a global minimum is rank-deficient by at least the order of $1 - 1/L$, where L is the

depth of the network. Moreover, they showed that the sharpness of the flattest minima increases approximately linearly with L if $L \gg 1$. Singh & Hofmann (2024) provided a full characterization of the Hessian spectrum at a point in parameter space for linear and ReLU networks in the *scalar regression* case. They observed that the eigenvalues scale in proportion to the input variance within one hidden-layer scalar linear networks. More recently, Jozs (2025) has shown that locally flat minima are globally flat in depth-2 matrix factorization problems.

Balanced Minima. Ghosh et al. (2025) provided a full characterization of the Hessian spectrum at balanced minima in deep matrix factorization. Furthermore, they showed that the maximum eigenvalue of the Hessian at the flattest minima is equal to that of the balanced minima. Ding et al. (2024) showed that *norm-minimal*, *balanced*, and *flat* solutions coincide in depth-2 matrix factorization, where flatness/sharpness measured by the *scaled trace* of the Hessian matrix of loss function. Wang et al. (2022) showed that large step size GD training induces a *balancing effect* between factors in depth-2 matrix factorization.

Dynamical Stability. In dynamical systems theory, it is well established that asymptotic convergence to a critical point is determined solely by the local stability of that point (Strogatz, 2024). In the seminal work of Wu et al. (2018) on the dynamical stability analysis of GD training, it was shown that a global minimum is *dynamically stable* for GD if and only if the step size does not exceed $2/\lambda_{\max}$. Mulayoff et al. (2021) investigated this mechanism in the space of learned functions for two-layer overparameterized univariate ReLU networks in the interpolation regime. This was then extended to multivariate ReLU networks by Nacson et al. (2023). The interpolation assumption was then removed by Qiao et al. (2024); Liang et al. (2025).

Edge-of-Stability. Cohen et al. (2021) observed that neural networks trained with GD typically operate in a regime called *edge of stability*, in which the maximum eigenvalue of the Hessian of loss function hovers just above the value $2/\eta$, where η is the step size, and argued that classical optimization theory fails to explain this phenomenon. Recently, Liang et al. (2025) empirically observed that explicit regularization seems to break the edge-of-stability phenomenon.

Flatness/Sharpness and Generalization. It is widely recognized in the literature that flat minima are associated with better generalization (Hochreiter & Schmidhuber, 1997; Keskar et al., 2017). In a large-scale empirical investigation, Jiang et al. (2020) examined different measures for deep networks and found that a sharpness-based measure exhibited the strongest correlation with generalization. There is also theoretical evidence for this phenomenon in low-rank matrix recovery (Ding et al., 2024). On the other hand, Dinh et al. (2017) showed that *good minima* can be arbitrarily sharp in deep neural networks.

2 NOTATION, PRELIMINARIES, AND PROBLEM SETUP

We denote the *Kronecker product* by \otimes , the *Frobenius inner product* by $\langle \cdot, \cdot \rangle$, the *spectral norm* by $\sigma_{\max}(\cdot)$, and the *Frobenius norm* by $\|\cdot\|_F$. We denote by $[L]$ the set of natural numbers up to L , i.e., $[L] = \{1, 2, \dots, L\}$.

To simplify the notation for subsequent derivations, we define

$$\prod_{j=n}^m \mathbf{W}_j := \begin{cases} \mathbf{W}_m \mathbf{W}_{m-1} \dots \mathbf{W}_n & \text{if } n \leq m, \\ \mathbf{I}_{d_m} & \text{otherwise, where } n, m \in [L], \end{cases} \quad (3)$$

where $\mathbf{W}_m \in \mathbb{R}^{d_m \times d_{m-1}}$.

Our analysis relies on matrix calculus and the formulation of directional second derivatives. Therefore, before proceeding to the technical details, we find it useful to first develop the intuition behind directional derivatives of real-valued functions of matrix variables.

Gâteaux Derivatives. Let $f : \mathbb{R}^{K \times L} \rightarrow \mathbb{R}$ be a differentiable function with continuous first- and second-order derivatives on $\mathbb{R}^{K \times L}$. Our objective is to derive closed-form expressions for the first- and second-order directional derivatives of f in the direction of $\mathbf{U} \in \mathbb{R}^{K \times L}$, where $\|\mathbf{U}\|_F < \infty$, denoted respectively by $D_{\mathbf{U}}f(\mathbf{X})$ and $D_{\mathbf{U}}^2f(\mathbf{X})$. By the limit definition of the derivative, the first derivative of $f(\mathbf{X})$ with respect to each entry of \mathbf{X} can be expressed as follows:

$$\frac{\partial f(\mathbf{X})}{\partial X_{ij}} = \lim_{\Delta t \rightarrow 0} \frac{f(\mathbf{X} + \Delta t \mathbf{e}_i \mathbf{e}_j^\top) - f(\mathbf{X})}{\Delta t}, \quad \forall (i, j) \in [K] \times [L], \quad (4)$$

where \mathbf{e}_i is the i^{th} standard basis vector of \mathbb{R}^K and \mathbf{e}_j is the j^{th} standard basis vector of \mathbb{R}^L . If the limit in (4) exists then by substitution of variables

$$\frac{\partial f(\mathbf{X})}{\partial X_{ij}} U_{ij} = \lim_{\Delta t \rightarrow 0} \frac{f(\mathbf{X} + \Delta t U_{ij} \mathbf{e}_i \mathbf{e}_j^\top) - f(\mathbf{X})}{\Delta t}, \quad \forall (i, j) \in [K] \times [L]. \quad (5)$$

By definition, the total change in $f(\mathbf{X})$ in the direction of \mathbf{U} is the sum of change due to each entry of \mathbf{X} . Then

$$D_{\mathbf{U}} f(\mathbf{X}) = \sum_{i,j \in [k] \times [l]} \frac{\partial f(\mathbf{X})}{\partial X_{ij}} U_{ij} \quad (6)$$

$$= \sum_{i,j \in [k] \times [l]} \lim_{\Delta t \rightarrow 0} \frac{f(\mathbf{X} + \Delta t U_{ij} \mathbf{e}_i \mathbf{e}_j^\top) - f(\mathbf{X})}{\Delta t} \quad (7)$$

$$= \lim_{\Delta t \rightarrow 0} \frac{f(\mathbf{X} + \Delta t \mathbf{U}) - f(\mathbf{X})}{\Delta t}. \quad (8)$$

We can rewrite the (8) as follows:

$$\lim_{\Delta t \rightarrow 0} \left. \frac{f(\mathbf{X} + (\Delta t + t)\mathbf{U}) - f(\mathbf{X} + t\mathbf{U})}{\Delta t} \right|_{t=0} = \left. \frac{\partial f(\mathbf{X} + t\mathbf{U})}{\partial t} \right|_{t=0}. \quad (9)$$

This is known as the *Gâteaux derivative*, which represents the change in $f(\mathbf{X})$ under a perturbation in the direction of \mathbf{U} . By the same reasoning, we obtain the following result.

Lemma 2. *The second directional derivative of f at \mathbf{X} in the direction $\mathbf{U} \in \mathbb{R}^{K \times L}$ is given by*

$$D_{\mathbf{U}}^2 f(\mathbf{X}) = \left. \frac{\partial^2}{\partial t^2} f(\mathbf{X} + t\mathbf{U}) \right|_{t=0}. \quad (10)$$

The proof is deferred to Appendix A.1.

Directional Second Derivatives and Maximum Eigenvalue. Consider the following objective function for our real-valued matrix-variable function f .

$$f(\mathbf{W}_1, \mathbf{W}_2, \dots, \mathbf{W}_L) = \|\mathbf{M} - \mathbf{W}_L \mathbf{W}_{L-1} \cdots \mathbf{W}_1\|_F^2, \quad (11)$$

where $\mathbf{W}_i \in \mathbb{R}^{d_i \times d_{i-1}}$ and $\mathbf{M} \in \mathbb{R}^{d_L \times d_0}$ for all $i \in [L]$. In this setting, we can define the largest eigenvalue of the $\nabla^2 f(\mathbf{W}_1, \mathbf{W}_2, \dots, \mathbf{W}_L)$ at an arbitrary point in the parameter space as follows:

$$\lambda_{\max}(\nabla^2 f(\mathbf{W}_1, \mathbf{W}_2, \dots, \mathbf{W}_L)) = \max_{\substack{\mathbf{U}_1, \mathbf{U}_2, \dots, \mathbf{U}_L \\ \sum_{i=1}^L \|\mathbf{U}_i\|_F^2 = 1}} \left. \frac{d^2}{dt^2} f(\mathbf{W}_1 + t\mathbf{U}_1, \dots, \mathbf{W}_L + t\mathbf{U}_L) \right|_{t=0}. \quad (12)$$

This is the generalization of the Rayleigh quotient to the case where the Hessian is represented as a tensor and its eigenvectors take the form of matrices. This leads to the following lemma.

Lemma 3. *For any $[\mathbf{W}_1^*, \mathbf{W}_2^*, \dots, \mathbf{W}_L^*]$ such that $\mathbf{M} = \prod_{j=1}^L \mathbf{W}_j^*$, the directional second derivative is given by*

$$\nabla^2 f(\mathbf{W}_1^*, \dots, \mathbf{W}_L^*)[\mathbf{U}_1, \dots, \mathbf{U}_L] = 2 \left\| \sum_{i=1}^L \left[\left(\prod_{j=i+1}^L \mathbf{W}_j^* \right) \mathbf{U}_i \left(\prod_{j=1}^{i-1} \mathbf{W}_j^* \right) \right] \right\|_F^2. \quad (13)$$

The proof is deferred to Appendix A.2.

We study the sharpness of the loss landscape near any global minimum in deep matrix factorization problems. We consider the following optimization problem

$$\min_{\mathbf{w} \in \mathbb{R}^N} \mathcal{L}(\mathbf{w}) := \|\mathbf{M} - \mathbf{W}_L \mathbf{W}_{L-1} \cdots \mathbf{W}_1\|_F^2, \quad (14)$$

where $\mathbf{w} = \text{vec}([\mathbf{W}_1, \mathbf{W}_2, \dots, \mathbf{W}_L])$ denotes the collection of all parameters, and

$$N := \sum_{i=1}^L d_i \times d_{i-1} \quad (15)$$

is the total number of parameters in the model. $\mathbf{M} \in \mathbb{R}^{d_L \times d_0}$ denotes the optimal parameters, $L \geq 2$ denotes the depth of factorization and $\mathbf{W}_i \in \mathbb{R}^{d_i \times d_{i-1}}$ is the i^{th} factor (layer). This objective is analogous to that of deep linear neural networks. To guarantee the feasibility of factorization at all points in $\mathbb{R}^{d_L \times d_0}$, we require

$$\min_i d_i \geq \min\{d_0, d_L\} \quad \forall i \in [L], \quad (16)$$

which follows directly from the fact that

$$\text{rank}(\mathbf{W}_L \mathbf{W}_{L-1} \cdots \mathbf{W}_1) \leq \min\{\text{rank}(\mathbf{W}_1), \text{rank}(\mathbf{W}_2), \dots, \text{rank}(\mathbf{W}_L)\}. \quad (17)$$

Define the set of global minima of $\mathcal{L}(\mathbf{w})$ as

$$\Omega := \arg \min_{\mathbf{w} \in \mathbb{R}^N} \mathcal{L}(\mathbf{w}) = \left\{ \mathbf{w} \in \mathbb{R}^N : \prod_{i=1}^L \mathbf{W}_i = \mathbf{M} \right\}. \quad (18)$$

3 WARM-UP: DEEP OVERPARAMETERIZED SCALAR FACTORIZATION

Before we delve into our general results, we first investigate the deep overparameterized scalar factorization, i.e., a special case of deep matrix factorization in which the first and last layers are vectors. This simplified problem setup reveals the key proof techniques used to prove our general result in Section 4.

Theorem 4. *Consider the following objective function*

$$\mathcal{L}(\mathbf{w}) := (m - \mathbf{w}_L \mathbf{W}_{L-1} \cdots \mathbf{W}_2 \mathbf{w}_1)^2, \quad (19)$$

where $m \in \mathbb{R}$, $d_0 = d_L = 1$, $\mathbf{w}_L \in \mathbb{R}^{1 \times d_{L-1}}$ and $\mathbf{w}_1 \in \mathbb{R}^{d_1 \times 1}$. For hidden factors (layers), i.e. for all $i \in \{2, 3, \dots, L-1\}$, we have $\mathbf{W}_i \in \mathbb{R}^{d_i \times d_{i-1}}$. Then, $\forall \mathbf{w}^* \in \Omega$,

$$\lambda_{\max}(\nabla^2 \mathcal{L}(\mathbf{w}^*)) = 2 \sum_{i=1}^L \sigma_{\max} \left(\prod_{j=i+1}^L \mathbf{W}_j^* \right)^2 \sigma_{\max} \left(\prod_{j=1}^{i-1} \mathbf{W}_j^* \right)^2. \quad (20)$$

Proof. According to (12) and (13),

$$\lambda_{\max}(\nabla^2 \mathcal{L}(\mathbf{w}^*)) = \max_{\substack{\mathbf{U}_1, \mathbf{U}_2, \dots, \mathbf{U}_L: \\ \sum_{i=1}^L \|\mathbf{U}_i\|_F^2 = 1}} 2 \left\| \sum_{i=1}^L \left[\left(\prod_{j=i+1}^L \mathbf{W}_j^* \right) \mathbf{U}_i \left(\prod_{j=1}^{i-1} \mathbf{W}_j^* \right) \right] \right\|_F^2 \quad (21)$$

$$\leq \max_{\substack{\mathbf{U}_1, \mathbf{U}_2, \dots, \mathbf{U}_L: \\ \sum_{i=1}^L \|\mathbf{U}_i\|_F^2 = 1}} 2 \left(\sum_{i=1}^L \left\| \left(\prod_{j=i+1}^L \mathbf{W}_j^* \right) \mathbf{U}_i \left(\prod_{j=1}^{i-1} \mathbf{W}_j^* \right) \right\|_F \right)^2 \quad (22)$$

$$= \max_{\substack{\mathbf{u}_1, \mathbf{u}_2, \dots, \mathbf{u}_L: \\ \sum_{i=1}^L \|\mathbf{u}_i\|_2^2 = 1}} 2 \left(\sum_{i=1}^L \left\| \left[\left(\prod_{j=1}^{i-1} \mathbf{W}_j^* \right)^\top \otimes \left(\prod_{j=i+1}^L \mathbf{W}_j^* \right) \right] \mathbf{u}_i \right\|_2 \right)^2 \quad (23)$$

$$\leq \max_{\substack{\mathbf{u}_1, \mathbf{u}_2, \dots, \mathbf{u}_L: \\ \sum_{i=1}^L \|\mathbf{u}_i\|_2^2 = 1}} 2 \left(\sum_{i=1}^L \sigma_{\max} \left(\left(\prod_{j=1}^{i-1} \mathbf{W}_j^* \right)^\top \otimes \left(\prod_{j=i+1}^L \mathbf{W}_j^* \right) \right) \|\mathbf{u}_i\|_2 \right)^2 \quad (24)$$

$$= \max_{\substack{\mathbf{u}_1, \mathbf{u}_2, \dots, \mathbf{u}_L: \\ \sum_{i=1}^L \|\mathbf{u}_i\|_2^2 = 1}} 2 \left(\sum_{i=1}^L \sigma_{\max} \left(\prod_{j=i+1}^L \mathbf{W}_j^* \right) \sigma_{\max} \left(\prod_{j=1}^{i-1} \mathbf{W}_j^* \right) \|\mathbf{u}_i\|_2 \right)^2. \quad (25)$$

We can upper bound the right-hand side of (21) by using the *triangle inequality*. By applying the *vectorization trick* of the Kronecker product, we can rewrite (22). Then, noting the fact that for any matrix $\mathbf{A} \in \mathbb{R}^{m \times n}$ and vector $\mathbf{x} \in \mathbb{R}^n$, $\|\mathbf{A}\mathbf{x}\|_2 \leq \sigma_{\max}(\mathbf{A})\|\mathbf{x}\|_2$, we can upper bound the right-hand side of (23). Note that for any matrix \mathbf{A} and \mathbf{B} , $\sigma_{\max}(\mathbf{A} \otimes \mathbf{B}) = \sigma_{\max}(\mathbf{A})\sigma_{\max}(\mathbf{B})$. Hence, we can rewrite (24).

Since $\sum_{i=1}^L \sigma_{\max}\left(\prod_{j=i+1}^L \mathbf{W}_j^*\right) \sigma_{\max}\left(\prod_{j=1}^{i-1} \mathbf{W}_j^*\right) \|\mathbf{u}_i\|_2 \geq 0$ for all \mathbf{u}_i such that $\sum_{i=1}^L \|\mathbf{u}_i\|_2^2 = 1$, we can write the following equivalence

$$\arg \max_{\substack{\mathbf{u}_1, \mathbf{u}_2, \dots, \mathbf{u}_L: \\ \sum_{i=1}^L \|\mathbf{u}_i\|_2^2 = 1}} 2 \left(\sum_{i=1}^L \sigma_{\max}\left(\prod_{j=i+1}^L \mathbf{W}_j^*\right) \sigma_{\max}\left(\prod_{j=1}^{i-1} \mathbf{W}_j^*\right) \|\mathbf{u}_i\|_2 \right)^2 \quad (26)$$

$$= \arg \max_{\substack{\mathbf{u}_1, \mathbf{u}_2, \dots, \mathbf{u}_L: \\ \sum_{i=1}^L \|\mathbf{u}_i\|_2^2 = 1}} 2 \sum_{i=1}^L \sigma_{\max}\left(\prod_{j=i+1}^L \mathbf{W}_j^*\right) \sigma_{\max}\left(\prod_{j=1}^{i-1} \mathbf{W}_j^*\right) \|\mathbf{u}_i\|_2. \quad (27)$$

This constrained optimization problem is a specific case of the following general constrained optimization problem.

$$\min_{\mathbf{x} \in \mathbb{R}_+^L} -\mathbf{c}^\top \mathbf{x} \quad \text{s.t.} \quad \|\mathbf{x}\|_2^2 \leq 1, \quad (28)$$

where $\mathbf{c} \geq \mathbf{0}$. Notice that this is a convex optimization problem. Moreover, it is straightforward to verify that the optimal solution must have unit norm. To solve it, we can formulate the Lagrangian as follows:

$$L(\mathbf{x}, \mu) = -\mathbf{c}^\top \mathbf{x} + \mu(\mathbf{x}^\top \mathbf{x} - 1) \quad \mu \geq 0. \quad (29)$$

We know that optimal solution satisfies KKT conditions. Therefore,

$$-\mathbf{c} + 2\mu\mathbf{x}^* = 0 \rightarrow \mathbf{x}^* = \frac{\mathbf{c}}{2\mu} \rightarrow \mathbf{x}^* = \frac{\mathbf{c}}{\|\mathbf{c}\|_2}. \quad (30)$$

If you select

$$\mathbf{c} = \begin{bmatrix} \sigma_{\max}\left(\prod_{j=2}^L \mathbf{W}_j^*\right) \\ \sigma_{\max}\left(\prod_{j=3}^L \mathbf{W}_j^*\right) \sigma_{\max}\left(\mathbf{W}_1^*\right) \\ \vdots \\ \sigma_{\max}\left(\prod_{j=1}^{L-1} \mathbf{W}_j^*\right) \end{bmatrix} \quad (31)$$

then this implies

$$\begin{aligned} & \max_{\substack{\mathbf{u}_1, \mathbf{u}_2, \dots, \mathbf{u}_L: \\ \sum_{i=1}^L \|\mathbf{u}_i\|_2^2 = 1}} 2 \left(\sum_{i=1}^L \sigma_{\max}\left(\prod_{j=i+1}^L \mathbf{W}_j^*\right) \sigma_{\max}\left(\prod_{j=1}^{i-1} \mathbf{W}_j^*\right) \|\mathbf{u}_i\|_2 \right)^2 \\ &= 2 \sum_{i=1}^L \sigma_{\max}\left(\prod_{j=i+1}^L \mathbf{W}_j^*\right)^2 \sigma_{\max}\left(\prod_{j=1}^{i-1} \mathbf{W}_j^*\right)^2, \end{aligned} \quad (32)$$

and

$$\lambda_{\max}(\nabla^2 \mathcal{L}(\mathbf{w}^*)) \leq 2 \sum_{i=1}^L \sigma_{\max}\left(\prod_{j=i+1}^L \mathbf{W}_j^*\right)^2 \sigma_{\max}\left(\prod_{j=1}^{i-1} \mathbf{W}_j^*\right)^2. \quad (33)$$

Then, it suffices to show that there exists a direction $[\mathbf{U}_1^*, \mathbf{U}_2^*, \dots, \mathbf{U}_L^*]$ on hypersphere along which the bound in (33) is achieved.

Consider decomposition of $\prod_{j=i+1}^L \mathbf{W}_j^*$ by SVD, and denote by \mathbf{u}_{L_i} and \mathbf{v}_{L_i} the left and right singular vectors of $\prod_{j=i+1}^L \mathbf{W}_j^*$ corresponding to the largest singular value, respectively. Note that since \mathbf{W}_L is a vector, we have $\mathbf{u}_{L_i} = 1$ for all $i \in [L]$. Moreover, decompose $\prod_{j=1}^{i-1} \mathbf{W}_j^*$ by SVD, and denote by \mathbf{u}_{R_i} and \mathbf{v}_{R_i} the left and right singular vectors of $\prod_{j=1}^{i-1} \mathbf{W}_j^*$ corresponding to the largest singular value, respectively. Note that since \mathbf{W}_1 is a vector, we have $\mathbf{v}_{R_i} = 1$ for all $i \in [L]$.

Now, we determine a particular direction $[U_1^*, U_2^*, \dots, U_L^*]$ such that they achieve the upper bound while satisfying the constraint $\sum_{i=1}^L \|U_i^*\|_F^2 = 1$. Choose

$$U_i^* = \frac{\sigma_{\max}\left(\prod_{j=i+1}^L W_j^*\right) \sigma_{\max}\left(\prod_{j=1}^{i-1} W_j^*\right)}{\sqrt{\sum_{i=1}^L \sigma_{\max}\left(\prod_{j=i+1}^L W_j^*\right)^2 \sigma_{\max}\left(\prod_{j=1}^{i-1} W_j^*\right)^2}} v_{L_i} u_{R_i}^\top. \quad (34)$$

Then,

$$2 \left\| \sum_{i=1}^L \left[\left(\prod_{j=i+1}^L W_j^* \right) U_i^* \left(\prod_{j=1}^{i-1} W_j^* \right) \right] \right\|_F^2 = 2 \sum_{i=1}^L \sigma_{\max}\left(\prod_{j=i+1}^L W_j^*\right)^2 \sigma_{\max}\left(\prod_{j=1}^{i-1} W_j^*\right)^2. \quad (35)$$

Since the upper bound is achieved, it implies

$$\lambda_{\max}(\nabla^2 \mathcal{L}(w^*)) = 2 \sum_{i=1}^L \sigma_{\max}\left(\prod_{j=i+1}^L W_j^*\right)^2 \sigma_{\max}\left(\prod_{j=1}^{i-1} W_j^*\right)^2. \quad (36)$$

□

4 OVERPARAMETERIZED DEEP MATRIX FACTORIZATION

We now consider the general deep matrix factorization problem. In this section, we prove our main result, which is closed-form expression for the maximum eigenvalue of the Hessian for any global minimum to the objective (14).

Theorem 5. *If $w^* \in \Omega$ then*

$$\lambda_{\max}(\nabla^2 \mathcal{L}(w^*)) = 2 \sigma_{\max}\left(\sum_{i=1}^L B_i^\top B_i \otimes A_i A_i^\top\right), \quad (37)$$

where $A_k = \prod_{i=k+1}^L W_i^*$ and $B_k = \prod_{i=1}^{k-1} W_i^*$.

The proof appears in Appendix B.1. Note that the deep overparameterized scalar factorization is a special case of deep matrix factorization where both $B_i^\top B_i$ and $A_i A_i^\top$ reduce to scalars. In that special case, we recover Theorem 4. Another corollary of Theorem 5 is the maximum Hessian eigenvalue for the classical (depth-2) matrix factorization problem. This result may be of independent interest as the expression simplifies considerably.

Corollary 6. *Consider the following depth-2 matrix factorization objective*

$$\mathcal{L}(L, R) = \|M - LR^\top\|_F^2, \quad (38)$$

where $M \in \mathbb{R}^{d_L \times d_0}$ is the optimal parameters and $L \in \mathbb{R}^{d_L \times k}$, $R \in \mathbb{R}^{d_0 \times k}$. To ensure the feasibility of the factorization every point in $\mathbb{R}^{d_L \times d_0}$, we choose $k \geq \min\{d_0, d_L\}$. We define the set of minimizers as follows:

$$\Omega := \arg \min_{L, R} \mathcal{L}(L, R) = \{(L, R) : M = LR^\top\}. \quad (39)$$

If $(L, R) \in \Omega$ then

$$\lambda_{\max}(\nabla^2 \mathcal{L}(L, R)) = 2(\sigma_{\max}(L)^2 + \sigma_{\max}(R)^2). \quad (40)$$

Proof. We have from Theorem 5 that

$$\lambda_{\max}(\nabla^2 \mathcal{L}(L, R)) = 2 \sigma_{\max}(I \otimes LL^\top + RR^\top \otimes I). \quad (41)$$

Using the fact from Horn & Johnson (1994, Theorem 4.4.5), we can write

$$2 \sigma_{\max}(I \otimes LL^\top + RR^\top \otimes I) = 2 \sigma_{\max}(I \otimes LL^\top) + 2 \sigma_{\max}(RR^\top \otimes I). \quad (42)$$

Note that for any matrix A and B , $\sigma_{\max}(A \otimes B) = \sigma_{\max}(A) \sigma_{\max}(B)$, and $\sigma_{\max}(AA^\top) = \sigma_{\max}(A^\top A) = \sigma_{\max}(A)^2$. Hence,

$$2(\sigma_{\max}(I \otimes LL^\top) + \sigma_{\max}(RR^\top \otimes I)) = 2(\sigma_{\max}(L)^2 + \sigma_{\max}(R)^2). \quad (43)$$

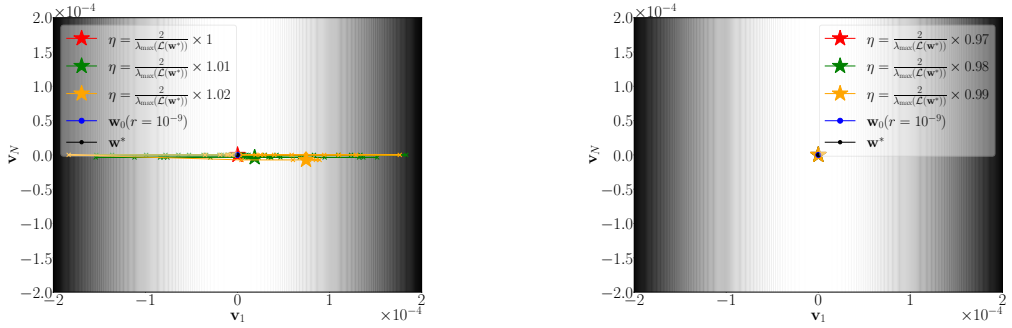
□

We also provide a self-contained proof of this corollary in Appendix B.2.

5 EXPERIMENTS

For the experiment, we first generate the layer dimensions randomly and then construct the optimal layers $[\mathbf{W}_1^*, \mathbf{W}_2^*, \dots, \mathbf{W}_L^*]$ as Gaussian random matrices, with each entry sampled from $N(0, 1)$ according to the generated dimensions. Then, we compute \mathbf{M} or m by $\prod_{j=1}^L \mathbf{W}_j^*$.

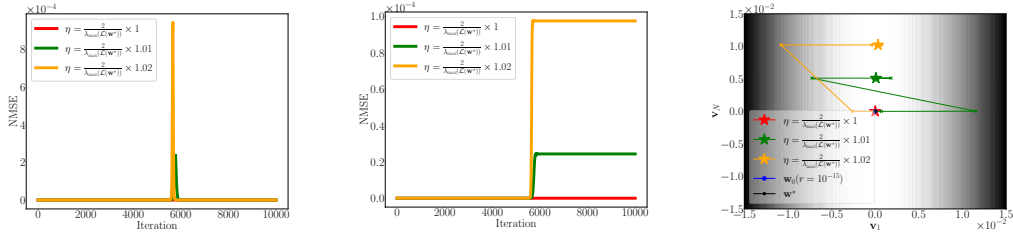
The linear stability analysis relies on a quadratic approximation of the loss function in the vicinity of a global minimum (Wu et al., 2018). To observe whether the escape phenomenon occurs, GD must be initialized at a locally attractive point. However, making a well-informed guess of such an initial point would require computing the third-order characteristics of the loss function, which is not feasible, since the third-order terms describe how rapidly the Hessian changes. Therefore, we initialize GD extremely close to the minimum—on the order of 10^{-15} to 10^{-9} —to ensure that it is initialized at a locally attractive point.



(a) Trajectories of GD initialized at \mathbf{w}_0 with step sizes $\geq 2/\lambda_{\max}$ are depicted by colored lines, and their corresponding convergence points are marked by colored \star symbols.

(b) Trajectories of GD initialized at \mathbf{w}_0 with step sizes $< 2/\lambda_{\max}$ are depicted by colored lines, and their corresponding convergence points are marked by colored \star symbols.

Figure 1: Contour map of the loss landscape around a minimum in a 15-layer overparameterized scalar factorization of a random scalar. GD with different step sizes η , indicated by different colors, is initialized within a radius of 10^{-9} from the minimum, in the direction of the Hessian eigenvector corresponding to the largest eigenvalue. The vector \mathbf{v}_1 denotes the eigenvector of the Hessian corresponding to the largest eigenvalue, while \mathbf{v}_N denotes the eigenvector corresponding to the smallest eigenvalue (see Appendix C.1). The value of $\lambda_{\max}(\nabla^2 \mathcal{L}(\mathbf{w}^*))$ is computed using the closed-form expression derived in Theorem 4.



(a) Normalized training error across iterations, i.e., $\mathcal{L}(\mathbf{w}_k) / \|\mathbf{M}\|_F^2$.

(b) Normalized ℓ^2 distance of \mathbf{w}_k from the minimum \mathbf{w}^* , i.e., $\|\mathbf{w}_k - \mathbf{w}^*\|_2^2 / \|\mathbf{w}^*\|_2^2$.

(c) Trajectories of GD on the contour map of the loss landscape around the minimum.

Figure 2: GD dynamics with different step sizes, $\eta \geq 2/\lambda_{\max}(\nabla^2 \mathcal{L}(\mathbf{w}^*))$, indicated by different colors, are initialized within a radius of 10^{-15} from the minimum in the direction of the Hessian eigenvector corresponding to the largest eigenvalue, for depth-2 matrix factorization, $\mathbf{M} = \mathbf{L}\mathbf{R}^\top$, of a random Gaussian matrix, where $\mathbf{L} \in \mathbb{R}^{10 \times 20}$ and $\mathbf{R} \in \mathbb{R}^{20 \times 20}$. The value of $\lambda_{\max}(\nabla^2 \mathcal{L}(\mathbf{w}^*))$ is computed using the closed-form expression derived in Corollary 6.

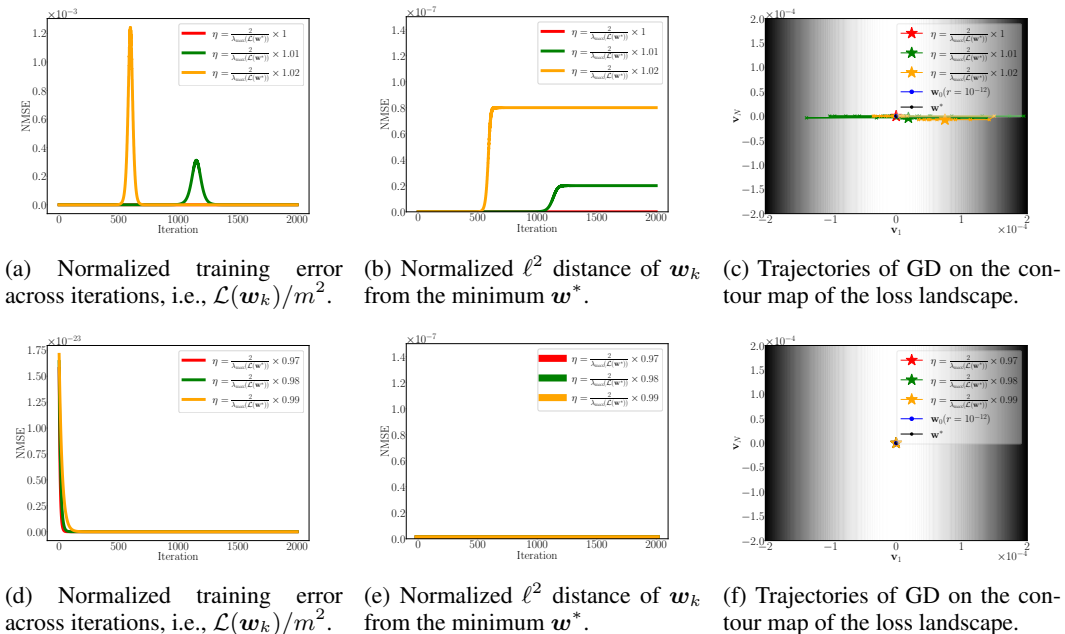


Figure 3: GD dynamics with different step sizes indicated by different colors are initialized within a radius of 10^{-12} from the minimum in the direction of the Hessian eigenvector corresponding to the largest eigenvalue, for a 15-layer overparameterized scalar factorization of a random scalar. The value of $\lambda_{\max}(\nabla^2\mathcal{L}(\mathbf{w}^*))$ is computed using the closed-form expression derived in Theorem 4.

To measure the distance between the convergence point and the minimizer, we plot the normalized ℓ^2 -norm of $\mathbf{w}_k - \mathbf{w}^*$ at each iteration. Furthermore, as shown in Fig. 1a, Figs. 2a, 3a and Figs. 2b, 3b, if $\eta > 2/\lambda_{\max}$, where $\lambda_{\max} := \lambda_{\max}(\nabla^2\mathcal{L}(\mathbf{w}^*))$, GD always escapes from the minimum, regardless of how close it is initialized to that point. On the other hand, if $\eta = 2/\lambda_{\max}$ then GD converges as shown in Figs. 1-3. A catapult in the training error indicates GD’s escape from the basin of a minimum, after which it eventually converges to another minimum as observed by Wu et al. (2018). For additional experiments, see Appendix C.2.

We choose the perturbation direction for the initial point to be the eigenvector of $\nabla^2\mathcal{L}(\mathbf{w}^*)$ corresponding to the largest eigenvalue, so as to avoid the manifold formed by minimizers as observed in Fig. 2c. For the methodology used to generate contour maps of the loss landscape and to track the trajectories of GD, see Appendix C.1.

6 CONCLUSION AND DISCUSSION

In this paper, we derived an exact expression for the maximum eigenvalue of the Hessian of the squared-error loss for deep matrix factorization problems for any global minimizer. Our experiments demonstrated that the escape phenomenon explored by Wang et al. (2022) in a one-dimensional problem also occurs in deep matrix factorization. Our results also directly extend to deep linear neural network training problems. Furthermore, the results of this paper provide a step towards understanding the implicit biases of gradient-based optimization methods for non-convex problems. It has been empirically observed that explicit regularization prevents the edge-of-stability phenomenon (Liang et al., 2025, Figure 3). Thus, it would be interesting to derive an exact expression for the maximum eigenvalue of the Hessian for the ℓ^2 -regularized deep matrix factorization problem.

REFERENCES

- Sanjeev Arora, Nadav Cohen, Wei Hu, and Yuping Luo. Implicit regularization in deep matrix factorization. *Advances in neural information processing systems*, 32, 2019.
- Peter L Bartlett, Philip M Long, Gábor Lugosi, and Alexander Tsigler. Benign overfitting in linear regression. *Proceedings of the National Academy of Sciences*, 117(48):30063–30070, 2020.
- Mikhail Belkin, Alexander Rakhlin, and Alexandre B Tsybakov. Does data interpolation contradict statistical optimality? In *The 22nd international conference on artificial intelligence and statistics*, pp. 1611–1619. PMLR, 2019.
- Jeremy Cohen, Simran Kaur, Yuanzhi Li, J Zico Kolter, and Ameet Talwalkar. Gradient descent on neural networks typically occurs at the edge of stability. In *International Conference on Learning Representations*, 2021.
- Lijun Ding, Dmitriy Drusvyatskiy, Maryam Fazel, and Zaid Harchaoui. Flat minima generalize for low-rank matrix recovery. *Information and Inference: A Journal of the IMA*, 13(2):iaae009, 2024.
- Laurent Dinh, Razvan Pascanu, Samy Bengio, and Yoshua Bengio. Sharp minima can generalize for deep nets. In *International Conference on Machine Learning*, pp. 1019–1028. PMLR, 2017.
- Spencer Frei, Niladri S Chatterji, and Peter Bartlett. Benign overfitting without linearity: Neural network classifiers trained by gradient descent for noisy linear data. In *Conference on Learning Theory*, pp. 2668–2703. PMLR, 2022.
- Avrajit Ghosh, Soo Min Kwon, Rongrong Wang, Saiprasad Ravishankar, and Qing Qu. Learning dynamics of deep matrix factorization beyond the edge of stability. In *The Thirteenth International Conference on Learning Representations*, 2025.
- Ian J Goodfellow, Oriol Vinyals, and Andrew M Saxe. Qualitatively characterizing neural network optimization problems. *arXiv preprint arXiv:1412.6544*, 2014.
- Suriya Gunasekar, Blake E Woodworth, Srinadh Bhojanapalli, Behnam Neyshabur, and Nati Srebro. Implicit regularization in matrix factorization. *Advances in neural information processing systems*, 30, 2017.
- Suriya Gunasekar, Jason D Lee, Daniel Soudry, and Nati Srebro. Implicit bias of gradient descent on linear convolutional networks. *Advances in neural information processing systems*, 31, 2018.
- Sepp Hochreiter and Jürgen Schmidhuber. Flat minima. *Neural computation*, 9(1):1–42, 1997.
- Roger A Horn and Charles R Johnson. *Topics in matrix analysis*. Cambridge university press, 1994.
- Ziwei Ji and Matus Telgarsky. Directional convergence and alignment in deep learning. *Advances in Neural Information Processing Systems*, 33:17176–17186, 2020.
- Yiding Jiang, Behnam Neyshabur, Hossein Mobahi, Dilip Krishnan, and Samy Bengio. Fantastic generalization measures and where to find them. In *International Conference on Learning Representations*, 2020.
- Cédric Jozz. On the geometry of flat minima, 2025.
- Nitish Shirish Keskar, Dheevatsa Mudigere, Jorge Nocedal, Mikhail Smelyanskiy, and Ping Tak Peter Tang. On large-batch training for deep learning: Generalization gap and sharp minima. In *International Conference on Learning Representations*, 2017.
- Alex Krizhevsky, Ilya Sutskever, and Geoffrey E Hinton. Imagenet classification with deep convolutional neural networks. *Advances in neural information processing systems*, 25, 2012.
- Hao Li, Zheng Xu, Gavin Taylor, Christoph Studer, and Tom Goldstein. Visualizing the loss landscape of neural nets. *Advances in neural information processing systems*, 31, 2018.
- Tongtong Liang, Dan Qiao, Yu-Xiang Wang, and Rahul Parhi. Stable minima of relu neural networks suffer from the curse of dimensionality: The neural shattering phenomenon. *arXiv preprint arXiv:2506.20779*, 2025.

-
- Chao Ma and Lexing Ying. On linear stability of sgd and input-smoothness of neural networks. *Advances in Neural Information Processing Systems*, 34:16805–16817, 2021.
- Rotem Mulayoff and Tomer Michaeli. Unique properties of flat minima in deep networks. In *International conference on machine learning*, pp. 7108–7118. PMLR, 2020.
- Rotem Mulayoff, Tomer Michaeli, and Daniel Soudry. The implicit bias of minima stability: A view from function space. *Advances in Neural Information Processing Systems*, 34:17749–17761, 2021.
- Mor Shpigel Nacson, Rotem Mulayoff, Greg Ongie, Tomer Michaeli, and Daniel Soudry. The implicit bias of minima stability in multivariate shallow relu networks. In *ICLR*, 2023.
- Kamil Nar and Shankar Sastry. Step size matters in deep learning. *Advances in Neural Information Processing Systems*, 31, 2018.
- Behnam Neyshabur, Ryota Tomioka, and Nathan Srebro. In search of the real inductive bias: On the role of implicit regularization in deep learning. *arXiv preprint arXiv:1412.6614*, 2014.
- Behnam Neyshabur, Srinadh Bhojanapalli, David McAllester, and Nati Srebro. Exploring generalization in deep learning. *Advances in neural information processing systems*, 30, 2017.
- Dan Qiao, Kaiqi Zhang, Esha Singh, Daniel Soudry, and Yu-Xiang Wang. Stable minima cannot overfit in univariate relu networks: Generalization by large step sizes. *Advances in Neural Information Processing Systems*, 37:94163–94208, 2024.
- Sidak Pal Singh and Thomas Hofmann. Closed form of the hessian spectrum for some neural networks. In *High-dimensional Learning Dynamics 2024: The Emergence of Structure and Reasoning*, 2024.
- Daniel Soudry, Elad Hoffer, Mor Shpigel Nacson, Suriya Gunasekar, and Nathan Srebro. The implicit bias of gradient descent on separable data. *Journal of Machine Learning Research*, 19(70): 1–57, 2018.
- Steven H Strogatz. *Nonlinear dynamics and chaos: with applications to physics, biology, chemistry, and engineering*. Chapman and Hall/CRC, 2024.
- Ashish Vaswani, Noam Shazeer, Niki Parmar, Jakob Uszkoreit, Llion Jones, Aidan N Gomez, Łukasz Kaiser, and Illia Polosukhin. Attention is all you need. *Advances in neural information processing systems*, 30, 2017.
- Yuqing Wang, Minshuo Chen, Tuo Zhao, and Molei Tao. Large learning rate tames homogeneity: Convergence and balancing effect. In *International Conference on Learning Representations*, 2022.
- Lei Wu, Chao Ma, et al. How sgd selects the global minima in over-parameterized learning: A dynamical stability perspective. *Advances in Neural Information Processing Systems*, 31, 2018.
- Chulhee Yun, Shankar Krishnan, and Hossein Mobahi. A unifying view on implicit bias in training linear neural networks. In *International Conference on Learning Representations*, 2021.
- Chiyuan Zhang, Samy Bengio, Moritz Hardt, Benjamin Recht, and Oriol Vinyals. Understanding deep learning requires rethinking generalization. In *International Conference on Learning Representations*, 2017.
- Xingyu Zhu, Zixuan Wang, Xiang Wang, Mo Zhou, and Rong Ge. Understanding edge-of-stability training dynamics with a minimalist example. In *The Eleventh International Conference on Learning Representations*, 2023.

A PROOFS FROM SECTION 2

A.1 PROOF OF LEMMA 2

Proof. We can express the derivative of $\frac{\partial f(\mathbf{X})}{\partial X_{ij}}$ with respect to each entry of \mathbf{X} , using the limit definition of the derivative, as follows:

$$\frac{\partial^2 f(\mathbf{X})}{\partial X_{kl} \partial X_{ij}} = \frac{\partial}{\partial X_{kl}} \left(\frac{\partial f(\mathbf{X})}{\partial X_{ij}} \right) = \lim_{\Delta t \rightarrow 0} \frac{\partial f(\mathbf{X} + \Delta t \mathbf{e}_i \mathbf{e}_j^\top) - \partial f(\mathbf{X})}{\partial X_{kl} \Delta t}, \quad \forall (k, l) \in [K] \times [L] \quad (44)$$

which is equal to

$$\lim_{\Delta h, \Delta t \rightarrow 0} \frac{f(\mathbf{X} + \Delta t \mathbf{e}_i \mathbf{e}_j^\top + \Delta h \mathbf{e}_k \mathbf{e}_l^\top) - f(\mathbf{X} + \Delta t \mathbf{e}_i \mathbf{e}_j^\top) - f(\mathbf{X} + \Delta h \mathbf{e}_k \mathbf{e}_l^\top) + f(\mathbf{X})}{\Delta h \Delta t}. \quad (45)$$

By using the substitution of variables as if in (5),

$$\frac{\partial^2 f(\mathbf{X})}{\partial X_{kl} \partial X_{ij}} U_{ij} U_{kl} = \frac{\partial}{\partial X_{kl}} \left(\frac{\partial f(\mathbf{X})}{\partial X_{ij}} U_{ij} \right) U_{kl} = \lim_{\Delta t \rightarrow 0} \frac{\partial f(\mathbf{X} + \Delta t U_{ij} \mathbf{e}_i \mathbf{e}_j^\top) - \partial f(\mathbf{X})}{\partial X_{kl} \Delta t} U_{kl}. \quad (46)$$

Equivalently,

$$\lim_{\Delta h, \Delta t \rightarrow 0} \frac{f(\mathbf{X} + \Delta t U_{ij} \mathbf{e}_i \mathbf{e}_j^\top + \Delta h U_{kl} \mathbf{e}_k \mathbf{e}_l^\top) - f(\mathbf{X} + \Delta t U_{ij} \mathbf{e}_i \mathbf{e}_j^\top) - f(\mathbf{X} + \Delta h U_{kl} \mathbf{e}_k \mathbf{e}_l^\top) + f(\mathbf{X})}{\Delta h \Delta t}. \quad (47)$$

which can be proved by substitution of variables in (46). In turn, second order differential due to any $\mathbf{U} \in \mathbb{R}^{K \times L}$ is

$$D_{\mathbf{U}}^2 f(\mathbf{X}) = \sum_{i,j} \sum_{k,l} \frac{\partial^2 f(\mathbf{X})}{\partial X_{kl} \partial X_{ij}} U_{ij} U_{kl} = \left\langle \nabla \langle \nabla f(\mathbf{X}), \mathbf{U} \rangle, \mathbf{U} \right\rangle, \quad (48)$$

where

$$\nabla f(\mathbf{X}) = \begin{bmatrix} \frac{\partial f(\mathbf{X})}{\partial X_{11}} & \frac{\partial f(\mathbf{X})}{\partial X_{12}} & \cdots & \frac{\partial f(\mathbf{X})}{\partial X_{1L}} \\ \frac{\partial f(\mathbf{X})}{\partial X_{21}} & \frac{\partial f(\mathbf{X})}{\partial X_{22}} & \cdots & \frac{\partial f(\mathbf{X})}{\partial X_{2L}} \\ \vdots & \ddots & \cdots & \vdots \\ \frac{\partial f(\mathbf{X})}{\partial X_{K1}} & \frac{\partial f(\mathbf{X})}{\partial X_{K2}} & \cdots & \frac{\partial f(\mathbf{X})}{\partial X_{KL}} \end{bmatrix} \in \mathbb{R}^{K \times L}. \quad (49)$$

Equivalently,

$$D_{\mathbf{U}}^2 f(\mathbf{X}) = \sum_{k,l} \lim_{\Delta t \rightarrow 0} \frac{\partial f(\mathbf{X} + \Delta t \mathbf{U} \mathbf{e}_i \mathbf{e}_j^\top) - \partial f(\mathbf{X})}{\partial X_{kl} \Delta t} U_{kl} \quad (50)$$

$$= \lim_{\Delta t \rightarrow 0} \frac{f(\mathbf{X} + 2\Delta t \mathbf{U}) - 2f(\mathbf{X} + \Delta t \mathbf{U}) + f(\mathbf{X})}{\Delta t^2} \quad (51)$$

$$= \frac{\partial^2}{\partial t^2} f(\mathbf{X} + t\mathbf{U}) \Big|_{t=0}. \quad (52)$$

□

A.2 PROOF OF LEMMA 3

Proof. We can rewrite (11) through using the definition of *Frobenius inner product*

$$f(\mathbf{W}_1, \dots, \mathbf{W}_L) = \left\langle M - \prod_{i=1}^L \mathbf{W}_i, M - \prod_{i=1}^L \mathbf{W}_i \right\rangle. \quad (53)$$

Then

$$f(\mathbf{W}_1 + t\mathbf{U}_1, \dots, \mathbf{W}_L + t\mathbf{U}_L) = \left\langle M - \prod_{i=1}^L (\mathbf{W}_i + t\mathbf{U}_i), M - \prod_{i=1}^L (\mathbf{W}_i + t\mathbf{U}_i) \right\rangle. \quad (54)$$

Let's define $g : \mathbb{R} \rightarrow \mathbb{R}^{d_L \times d_0}$ such that

$$g(t) = M - \prod_{i=1}^L (\mathbf{W}_i + t\mathbf{U}_i), \quad f(\mathbf{W}_1 + t\mathbf{U}_1, \dots, \mathbf{W}_L + t\mathbf{U}_L) = \langle g(t), g(t) \rangle. \quad (55)$$

First, we need to differentiate $f(\mathbf{W}_1 + t\mathbf{U}_1, \dots, \mathbf{W}_L + t\mathbf{U}_L)$ w.r.t t . Using the fact that $\langle \mathbf{A}, \mathbf{B} \rangle = \text{tr}(\mathbf{A}^\top \mathbf{B})$, which simplifies the differentiation,

$$\frac{d}{dt} f(\mathbf{W}_1 + t\mathbf{U}_1, \dots, \mathbf{W}_L + t\mathbf{U}_L) = 2 \langle g(t), g'(t) \rangle. \quad (56)$$

$$\frac{d^2}{dt^2} f(\mathbf{W}_1 + t\mathbf{U}_1, \dots, \mathbf{W}_L + t\mathbf{U}_L) = 2 \langle g'(t), g'(t) \rangle + 2 \langle g(t), g''(t) \rangle. \quad (57)$$

Then, the directional second derivative $\nabla^2 f(\mathbf{W}_1, \dots, \mathbf{W}_L)[\mathbf{U}_1, \dots, \mathbf{U}_L]$ equals to

$$\left. \frac{d^2}{dt^2} f(\mathbf{W}_1 + t\mathbf{U}_1, \dots, \mathbf{W}_L + t\mathbf{U}_L) \right|_{t=0} = 2 \langle g'(0), g'(0) \rangle + 2 \langle g(0), g''(0) \rangle. \quad (58)$$

It is straightforward to differentiate $g(t)$ such that

$$g(0) = M - \prod_{i=1}^L \mathbf{W}_i, \quad (59)$$

$$g'(0) = - \sum_{i=1}^L \left[\left(\prod_{j=i+1}^L \mathbf{w}_j \right) \mathbf{U}_i \left(\prod_{j=1}^{i-1} \mathbf{w}_j \right) \right], \quad (60)$$

$$g''(0) = -2 \sum_{1 \leq k < i \leq L} \left[\left(\prod_{j=i+1}^L \mathbf{w}_j \right) \mathbf{U}_i \left(\prod_{j=k+1}^{i-1} \mathbf{w}_j \right) \mathbf{U}_k \left(\prod_{j=1}^{k-1} \mathbf{w}_j \right) \right]. \quad (61)$$

Therefore, for any $[\mathbf{W}_1, \mathbf{W}_2, \dots, \mathbf{W}_L]$ in parameter space

$$\nabla^2 f(\mathbf{W}_1, \dots, \mathbf{W}_L)[\mathbf{U}_1, \dots, \mathbf{U}_L] = \quad (62)$$

$$2 \left\langle \sum_{i=1}^L \left[\left(\prod_{j=i+1}^L \mathbf{w}_j \right) \mathbf{U}_i \left(\prod_{j=1}^{i-1} \mathbf{w}_j \right) \right], \sum_{i=1}^L \left[\left(\prod_{j=i+1}^L \mathbf{w}_j \right) \mathbf{U}_i \left(\prod_{j=1}^{i-1} \mathbf{w}_j \right) \right] \right\rangle \quad (63)$$

$$-4 \left\langle M - \prod_{i=1}^L \mathbf{w}_i, \sum_{1 \leq k < i \leq L} \left[\left(\prod_{j=i+1}^L \mathbf{w}_j \right) \mathbf{U}_i \left(\prod_{j=k+1}^{i-1} \mathbf{w}_j \right) \mathbf{U}_k \left(\prod_{j=1}^{k-1} \mathbf{w}_j \right) \right] \right\rangle. \quad (64)$$

Note that for any minimizer $[\mathbf{W}_1^*, \mathbf{W}_2^*, \dots, \mathbf{W}_L^*]$, $M - \prod_{j=1}^L \mathbf{W}_j^* = 0$. Hence, for any global minimum

$$\nabla^2 f(\mathbf{W}_1^*, \dots, \mathbf{W}_L^*)[\mathbf{U}_1, \dots, \mathbf{U}_L] = \quad (65)$$

$$2 \left\langle \sum_{i=1}^L \left[\left(\prod_{j=i+1}^L \mathbf{w}_j^* \right) \mathbf{U}_i \left(\prod_{j=1}^{i-1} \mathbf{w}_j^* \right) \right], \sum_{i=1}^L \left[\left(\prod_{j=i+1}^L \mathbf{w}_j^* \right) \mathbf{U}_i \left(\prod_{j=1}^{i-1} \mathbf{w}_j^* \right) \right] \right\rangle. \quad (66)$$

□

B PROOFS FROM SECTION 4

B.1 PROOF OF THEOREM 5

Proof. By definition,

$$\lambda_{\max}(\mathcal{L}(\mathbf{w}^*)) = \max_{\mathbf{U}_1, \mathbf{U}_2, \dots, \mathbf{U}_L: \sum_{i=1}^L \|\mathbf{U}_i\|_F^2 = 1} 2 \left\| \sum_{i=1}^L \left[\left(\prod_{j=i+1}^L \mathbf{W}_j^* \right) \mathbf{U}_i \left(\prod_{j=1}^{i-1} \mathbf{W}_j^* \right) \right] \right\|_F^2 \quad (67)$$

$$= \max_{\mathbf{U}_1, \mathbf{U}_2, \dots, \mathbf{U}_L: \sum_{i=1}^L \|\mathbf{U}_i\|_F^2 = 1} 2 \left\| \text{vec} \left(\sum_{i=1}^L \left[\left(\prod_{j=i+1}^L \mathbf{W}_j^* \right) \mathbf{U}_i \left(\prod_{j=1}^{i-1} \mathbf{W}_j^* \right) \right] \right) \right\|_2^2 \quad (68)$$

$$= \max_{\mathbf{U}_1, \mathbf{U}_2, \dots, \mathbf{U}_L: \sum_{i=1}^L \|\mathbf{U}_i\|_F^2 = 1} 2 \left\| \sum_{i=1}^L \text{vec} \left(\left(\prod_{j=i+1}^L \mathbf{W}_j^* \right) \mathbf{U}_i \left(\prod_{j=1}^{i-1} \mathbf{W}_j^* \right) \right) \right\|_2^2 \quad (69)$$

$$= \max_{\mathbf{u}_1, \mathbf{u}_2, \dots, \mathbf{u}_L: \sum_{i=1}^L \|\mathbf{u}_i\|_2^2 = 1} 2 \left\| \sum_{i=1}^L \left[\left(\prod_{j=1}^{i-1} \mathbf{W}_j^* \right)^\top \otimes \left(\prod_{j=i+1}^L \mathbf{W}_j^* \right) \right] \mathbf{u}_i \right\|_2^2. \quad (70)$$

Note that vec is a linear operator. Therefore, (68) can be rewritten as (69). Then, by using the vectorization trick of the Kronecker product, we can obtain (70). Let's define a block matrix and a vector such that

$$\mathbf{K} = \left[\mathbf{I} \otimes \prod_{j=2}^L \mathbf{W}_j^* | \mathbf{W}_1^{*\top} \otimes \left(\prod_{j=3}^L \mathbf{W}_j^* \right) | \dots | \left(\prod_{j=1}^{L-1} \mathbf{W}_j^* \right)^\top \otimes \mathbf{I} \right], \quad (71)$$

$$\mathbf{u} = [\mathbf{u}_1^\top \quad \mathbf{u}_2^\top \quad \dots \quad \mathbf{u}_L^\top]^\top. \quad (72)$$

Then,

$$\lambda_{\max}(\mathcal{L}(\mathbf{w}^*)) = \max_{\mathbf{u}: \|\mathbf{u}\|_2 = 1} 2 \|\mathbf{K}\mathbf{u}\|_2^2 \quad (73)$$

$$= \sigma_{\max}(\mathbf{K}^\top \mathbf{K}). \quad (74)$$

Note that $\sigma_{\max}(\mathbf{K}^\top \mathbf{K}) = \sigma_{\max}(\mathbf{K}\mathbf{K}^\top)$. Note that for any two block matrices \mathbf{A} and \mathbf{B} such that

$$\mathbf{A} = [\mathbf{A}_1 \quad \mathbf{A}_2 \quad \dots \quad \mathbf{A}_L] \in \mathbb{R}^{M_1 \times d}, \quad \mathbf{B} = \begin{bmatrix} \mathbf{B}_1 \\ \vdots \\ \mathbf{B}_L \end{bmatrix} \in \mathbb{R}^{d \times M_2} \quad (75)$$

$$\mathbf{A}\mathbf{B} = \sum_{i=1}^L \mathbf{A}_i \mathbf{B}_i, \quad \mathbf{A}\mathbf{B} \in \mathbb{R}^{M_1 \times M_2}. \quad (76)$$

Furthermore, for any matrices $\mathbf{A}, \mathbf{B}, \mathbf{C}, \mathbf{D}$ such that the matrix products $\mathbf{A}\mathbf{B}$ and $\mathbf{C}\mathbf{D}$ are well defined, we have

$$(\mathbf{A} \otimes \mathbf{C})(\mathbf{B} \otimes \mathbf{D}) = \mathbf{A}\mathbf{B} \otimes \mathbf{C}\mathbf{D}. \quad (77)$$

Using the fact that $(\mathbf{A} \otimes \mathbf{C})^\top = \mathbf{A}^\top \otimes \mathbf{C}^\top$ together with the previous property, it follows that

$$\lambda_{\max}(\nabla^2 \mathcal{L}(\mathbf{w}^*)) = 2\sigma_{\max} \left(\sum_{i=1}^L \mathbf{B}_i^\top \mathbf{B}_i \otimes \mathbf{A}_i \mathbf{A}_i^\top \right), \quad (78)$$

where $\mathbf{A}_k = \prod_{i=k+1}^L \mathbf{W}_i^*$ and $\mathbf{B}_k = \prod_{i=1}^{k-1} \mathbf{W}_i^*$.

□

B.2 PROOF OF COROLLARY 6

Proof. According to (13), for any $(\mathbf{L}^*, \mathbf{R}^*) \in \Omega$

$$\nabla^2 \mathcal{L}(\mathbf{L}^*, \mathbf{R}^*)[\mathbf{U}, \mathbf{V}] = 2 \|\mathbf{L}^* \mathbf{U}^\top + \mathbf{V} \mathbf{R}^{*\top}\|_F^2. \quad (79)$$

Then,

$$\lambda_{\max}(\nabla^2 \mathcal{L}(\mathbf{L}^*, \mathbf{R}^*)) = \max_{\substack{\mathbf{U}, \mathbf{V} \\ \|\mathbf{U}\|_F^2 + \|\mathbf{V}\|_F^2 = 1}} 2 \|\mathbf{L}^* \mathbf{U}^\top + \mathbf{V} \mathbf{R}^{*\top}\|_F^2 \quad (80)$$

$$\leq \max_{\substack{\mathbf{U}, \mathbf{V} \\ \|\mathbf{U}\|_F^2 + \|\mathbf{V}\|_F^2 = 1}} 2 \left(\|\mathbf{L}^* \mathbf{U}^\top\|_F + \|\mathbf{V} \mathbf{R}^{*\top}\|_F \right)^2 \quad (81)$$

$$= \max_{\substack{\mathbf{u}, \mathbf{v} \\ \|\mathbf{u}\|_2^2 + \|\mathbf{v}\|_2^2 = 1}} 2 \left(\|(\mathbf{I} \otimes \mathbf{L}^*) \mathbf{u}\|_2 + \|(\mathbf{R}^* \otimes \mathbf{I}) \mathbf{v}\|_2 \right)^2 \quad (82)$$

$$\leq \max_{\substack{\mathbf{u}, \mathbf{v} \\ \|\mathbf{u}\|_2^2 + \|\mathbf{v}\|_2^2 = 1}} 2 \left(\sigma_{\max}(\mathbf{I} \otimes \mathbf{L}^*) \|\mathbf{u}\|_2 + \sigma_{\max}(\mathbf{R}^* \otimes \mathbf{I}) \|\mathbf{v}\|_2 \right)^2. \quad (83)$$

We can upper bound the right-hand side of (80) using the *triangle inequality*. By applying the *vectorization trick* of the Kronecker product again, we can rewrite (81). Then, noting that for any matrix $\mathbf{A} \in \mathbb{R}^{m \times n}$ and vector $\mathbf{x} \in \mathbb{R}^n$, $\|\mathbf{A}\mathbf{x}\|_2 \leq \sigma_{\max}(\mathbf{A})\|\mathbf{x}\|_2$, we can upper bound the right-hand side of (82). Note that for any matrix \mathbf{A} and \mathbf{B} , $\sigma_{\max}(\mathbf{A} \otimes \mathbf{B}) = \sigma_{\max}(\mathbf{A})\sigma_{\max}(\mathbf{B})$. Hence,

$$\lambda_{\max}(\nabla^2 \mathcal{L}(\mathbf{L}^*, \mathbf{R}^*)) \leq \max_{\substack{\mathbf{u}, \mathbf{v} \\ \|\mathbf{u}\|_2^2 + \|\mathbf{v}\|_2^2 = 1}} 2 \left(\sigma_{\max}(\mathbf{L}^*) \|\mathbf{u}\|_2 + \sigma_{\max}(\mathbf{R}^*) \|\mathbf{v}\|_2 \right)^2. \quad (84)$$

Since $\sigma_{\max}(\mathbf{L}^*) \|\mathbf{u}\|_2 + \sigma_{\max}(\mathbf{R}^*) \|\mathbf{v}\|_2 \geq 0 \forall \mathbf{u}, \mathbf{v} : \|\mathbf{u}\|_2^2 + \|\mathbf{v}\|_2^2 = 1$, we can write the following equivalence.

$$\arg \max_{\substack{\mathbf{u}, \mathbf{v} \\ \|\mathbf{u}\|_2^2 + \|\mathbf{v}\|_2^2 = 1}} 2 \left(\sigma_{\max}(\mathbf{L}^*) \|\mathbf{u}\|_2 + \sigma_{\max}(\mathbf{R}^*) \|\mathbf{v}\|_2 \right)^2 = \arg \max_{\substack{\mathbf{u}, \mathbf{v} \\ \|\mathbf{u}\|_2^2 + \|\mathbf{v}\|_2^2 = 1}} \sigma_{\max}(\mathbf{L}^*) \|\mathbf{u}\|_2 + \sigma_{\max}(\mathbf{R}^*) \|\mathbf{v}\|_2. \quad (85)$$

This constrained optimization problem is a specific case of the following general constrained optimization problem.

$$\min_{\mathbf{x} \in \mathbb{R}_+^2} -\mathbf{c}^\top \mathbf{x} \quad \text{s.t.} \quad \|\mathbf{x}\|_2^2 \leq 1, \quad (86)$$

where $\mathbf{c} \geq \mathbf{0}$. Notice that this is a convex optimization problem. Moreover, it is straightforward to verify that the optimal solution must lie on the boundary of the constraint. To solve it, we can formulate the Lagrangian as follows:

$$L(\mathbf{x}, \mu) = -\mathbf{c}^\top \mathbf{x} + \mu(\mathbf{x}^\top \mathbf{x} - 1) \quad \mu \geq 0. \quad (87)$$

We know that optimal solution satisfies KKT conditions. Therefore,

$$-\mathbf{c} + 2\mu \mathbf{x}^* = 0 \rightarrow \mathbf{x}^* = \frac{\mathbf{c}}{2\mu} \rightarrow \mathbf{x}^* = \frac{\mathbf{c}}{\|\mathbf{c}\|_2}. \quad (88)$$

If you select $\mathbf{c} = \begin{bmatrix} \sigma_{\max}(\mathbf{L}^*) \\ \sigma_{\max}(\mathbf{R}^*) \end{bmatrix}$ then $\mathbf{x}^* = \begin{bmatrix} \frac{\sigma_{\max}(\mathbf{L}^*)}{\sqrt{\sigma_{\max}(\mathbf{L}^*)^2 + \sigma_{\max}(\mathbf{R}^*)^2}} \\ \frac{\sigma_{\max}(\mathbf{R}^*)}{\sqrt{\sigma_{\max}(\mathbf{L}^*)^2 + \sigma_{\max}(\mathbf{R}^*)^2}} \end{bmatrix}$. This implies

$$\max_{\substack{\mathbf{u}, \mathbf{v} \\ \|\mathbf{u}\|_2^2 + \|\mathbf{v}\|_2^2 = 1}} 2 \left(\sigma_{\max}(\mathbf{L}^*) \|\mathbf{u}\|_2 + \sigma_{\max}(\mathbf{R}^*) \|\mathbf{v}\|_2 \right)^2 = 2 \left(\sigma_{\max}(\mathbf{L}^*)^2 + \sigma_{\max}(\mathbf{R}^*)^2 \right). \quad (89)$$

Therefore,

$$\lambda_{\max}(\nabla^2 \mathcal{L}(\mathbf{L}^*, \mathbf{R}^*)) = \max_{\substack{\mathbf{U}, \mathbf{V} \\ \|\mathbf{U}\|_F^2 + \|\mathbf{V}\|_F^2 = 1}} 2 \|\mathbf{L}^* \mathbf{U}^\top + \mathbf{V} \mathbf{R}^{*\top}\|_F^2 \leq 2 \left(\sigma_{\max}(\mathbf{L}^*)^2 + \sigma_{\max}(\mathbf{R}^*)^2 \right). \quad (90)$$

Now, we will show that this upper bound is achievable. Let us decompose \mathbf{L}^* as $\mathbf{U}_L \boldsymbol{\Sigma}_L \mathbf{V}_L^\top$ by SVD, and denote by \mathbf{u}_L and \mathbf{v}_L the left and right singular vectors corresponding to the largest singular value, respectively. Moreover, decompose \mathbf{R}^* as $\mathbf{U}_R \boldsymbol{\Sigma}_R \mathbf{V}_R^\top$ by SVD, and denote by \mathbf{u}_R and \mathbf{v}_R the left and right singular vectors corresponding to the largest singular value, respectively. We determine a particular $(\mathbf{U}^*, \mathbf{V}^*)$ such that it achieves the upper bound while satisfying the constraint $\|\mathbf{U}^*\|_F^2 + \|\mathbf{V}^*\|_F^2 = 1$. Choose

$$\mathbf{U}^{*\top} = \frac{\sigma_{\max}(\mathbf{L}^*)}{\sqrt{\sigma_{\max}(\mathbf{L}^*)^2 + \sigma_{\max}(\mathbf{R}^*)^2}} \mathbf{v}_L \mathbf{u}_R^\top, \quad \mathbf{V}^* = \frac{\sigma_{\max}(\mathbf{R}^*)}{\sqrt{\sigma_{\max}(\mathbf{L}^*)^2 + \sigma_{\max}(\mathbf{R}^*)^2}} \mathbf{u}_L \mathbf{v}_R^\top. \quad (91)$$

Using the fact that, for any vectors \mathbf{x} and \mathbf{y} $\|\mathbf{x}\mathbf{y}^\top\|_F^2 = \|\mathbf{x}\|_2^2 \|\mathbf{y}\|_2^2$,

$$2 \left\| \frac{(\sigma_{\max}(\mathbf{L}^*)^2 + \sigma_{\max}(\mathbf{R}^*)^2)}{\sqrt{\sigma_{\max}(\mathbf{L}^*)^2 + \sigma_{\max}(\mathbf{R}^*)^2}} \mathbf{u}_L \mathbf{u}_R^\top \right\|_F^2 = 2(\sigma_{\max}(\mathbf{L}^*)^2 + \sigma_{\max}(\mathbf{R}^*)^2). \quad (92)$$

□

C ADDITIONAL EXPERIMENTAL RESULTS

C.1 VISUALIZATION OF THE CONTOUR MAP OF THE LOSS LANDSCAPE

To study the dynamics of deep matrix factorization, we analyze the trajectories of GD. Previous works have visualized neural network loss landscapes to explore their highly non-convex and non-Euclidean structure (Goodfellow et al., 2014; Li et al., 2018). However, the high-dimensionality prevents full visualization. As a result, only 1-D (line) or 2-D (surface) visualizations are available. In this paper, we focus on contour maps of the loss landscape in the vicinity of a global minimum and a methodology employed in prior studies to generate them.

Contour Plots with Random Projections. We want to visualize the loss landscape around a global minimum $\mathbf{w}^* \in \mathbb{R}^N$. We select two random vectors, $\boldsymbol{\zeta}$ and $\boldsymbol{\gamma}$, from \mathbb{R}^N . Then, for any $K \subset \mathbb{R}^2$, we can define the function $p : K \rightarrow \mathbb{R}$:

$$p(x, y) = \mathcal{L}(\mathbf{w}^* + x\boldsymbol{\zeta} + y\boldsymbol{\gamma}), \quad \forall (x, y) \in K, \quad (93)$$

and plot p with the desired resolution.

Scale Invariance and Manifolds. Note that our loss function is *scale-invariant*, which means that for any nonzero scalar $c \in \mathbb{R}$, multiplying one layer by c and the next layer by $1/c$, or vice versa, yields the same end-to-end function. This phenomenon forms a manifold for global minimizers in the loss landscape (Dinh et al., 2017). Furthermore, we know that $\nabla^2 \mathcal{L}(\mathbf{w}^*)$ is rank-deficient by at least the order of $1 - 1/L$; that is, at least $1 - 1/L$ of the eigenvalues values of $\nabla^2 \mathcal{L}(\mathbf{w}^*)$ are zero (Mulayoff & Michaeli, 2020). This means that the ratio of the manifold dimension to the ambient space dimension increases as L grows.

Projection onto the Hessian Eigenvectors. If we use random projections in visualizations, plots might not be informative to track the optimization dynamics of GD due to the phenomenon caused by the scale invariance. To make contour maps as informative as possible, we choose $\boldsymbol{\zeta}$ and $\boldsymbol{\gamma}$ to be \mathbf{v}_1 and \mathbf{v}_N , respectively — the eigenvectors of the largest and smallest eigenvalues of $\nabla^2 \mathcal{L}(\mathbf{w}^*)$.

C.2 ADDITIONAL EXPERIMENTS

For the experiment, we first generate the layer dimensions randomly and then construct the optimal layers $[\mathbf{W}_1^* \mathbf{W}_2^* \dots \mathbf{W}_L^*]$. We then perform the same experiments as in Figs. 1–3, varying the depth, dimensions, and initialization distance r (as shown in Figs. 1–7). We note that oscillations occur along the eigenvector corresponding to the maximum eigenvalue of the Hessian. The dimensions of the factors, i.e., d_0, d_1, \dots, d_L , in Fig. 6 are given by 1, 9, 4, 8, 24, 16, 17, 11, 21, 3, 22, 3, 3, 15, 3, 18, 17, 16, 5, 12, 1, which implies $N = 2421$, while the dimensions of the factors in Fig. 7 are given by 1, 9, 4, 8, 1, which implies $N = 293$.

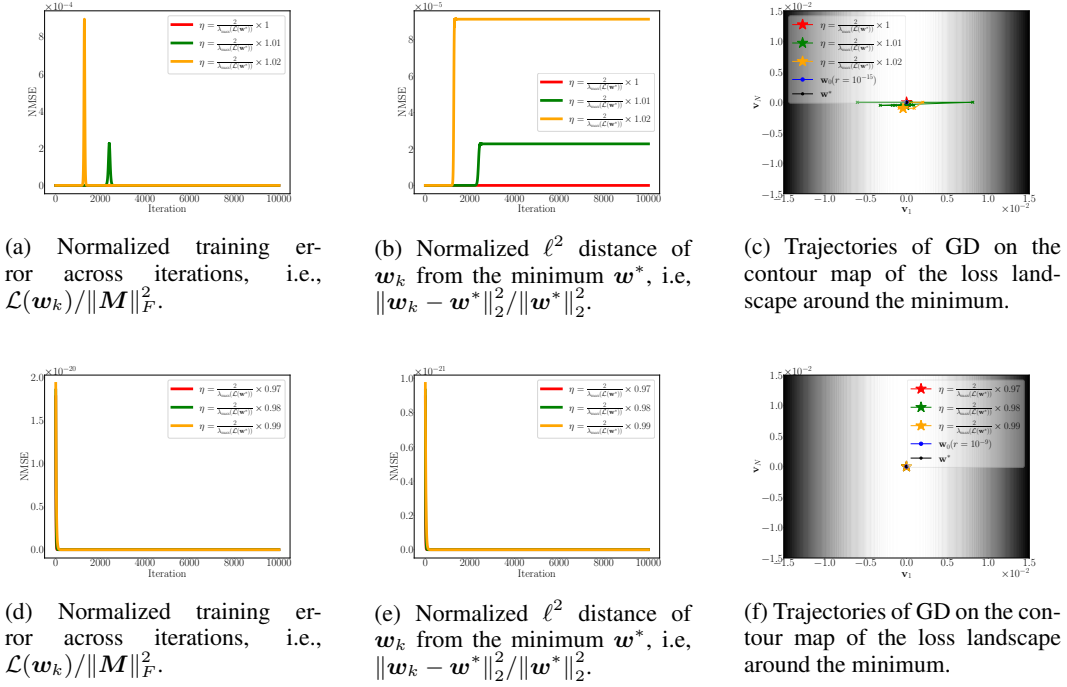


Figure 4: GD dynamics with different step sizes indicated by different colors for general matrix factorization, $\mathbf{M} = \mathbf{L}\mathbf{R}^\top$, of a random Gaussian matrix, where $\mathbf{L} \in \mathbb{R}^{10 \times 30}$ and $\mathbf{R} \in \mathbb{R}^{20 \times 30}$. The value of $\lambda_{\max}(\nabla^2 \mathcal{L}(\mathbf{w}^*))$ is computed using the closed-form expression derived in Corollary 6.

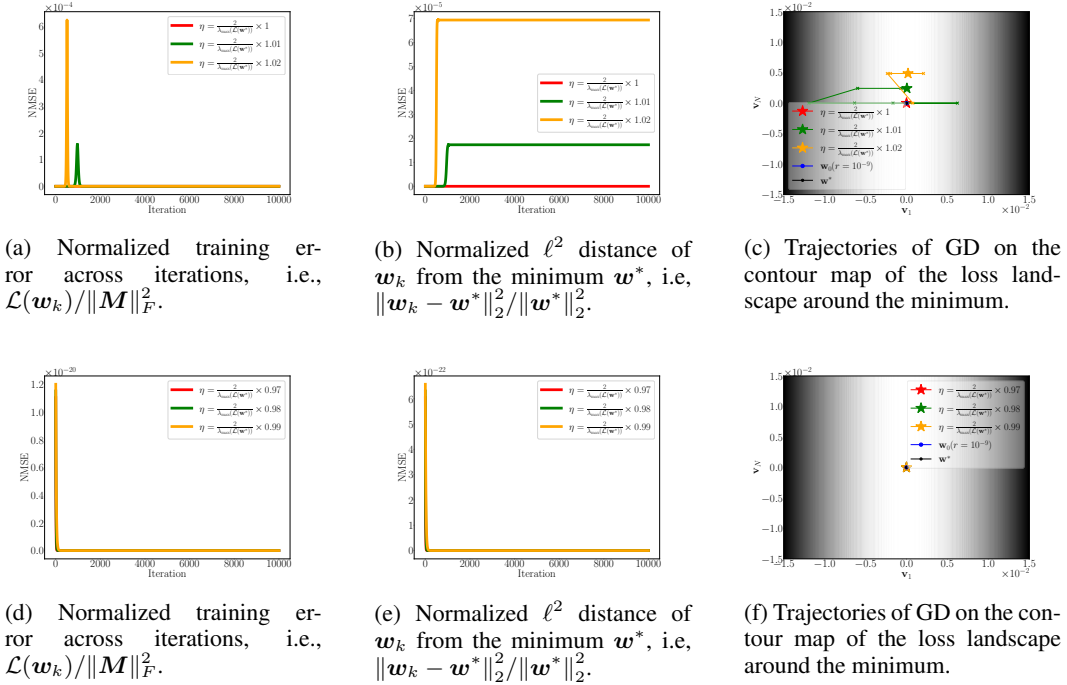


Figure 5: GD dynamics with different step sizes indicated by different colors for general matrix factorization, $\mathbf{M} = \mathbf{L}\mathbf{R}^\top$, of a random Gaussian matrix, where $\mathbf{L} \in \mathbb{R}^{25 \times 30}$ and $\mathbf{R} \in \mathbb{R}^{20 \times 30}$. The value of $\lambda_{\max}(\nabla^2 \mathcal{L}(\mathbf{w}^*))$ is computed using the closed-form expression derived in Corollary 6.

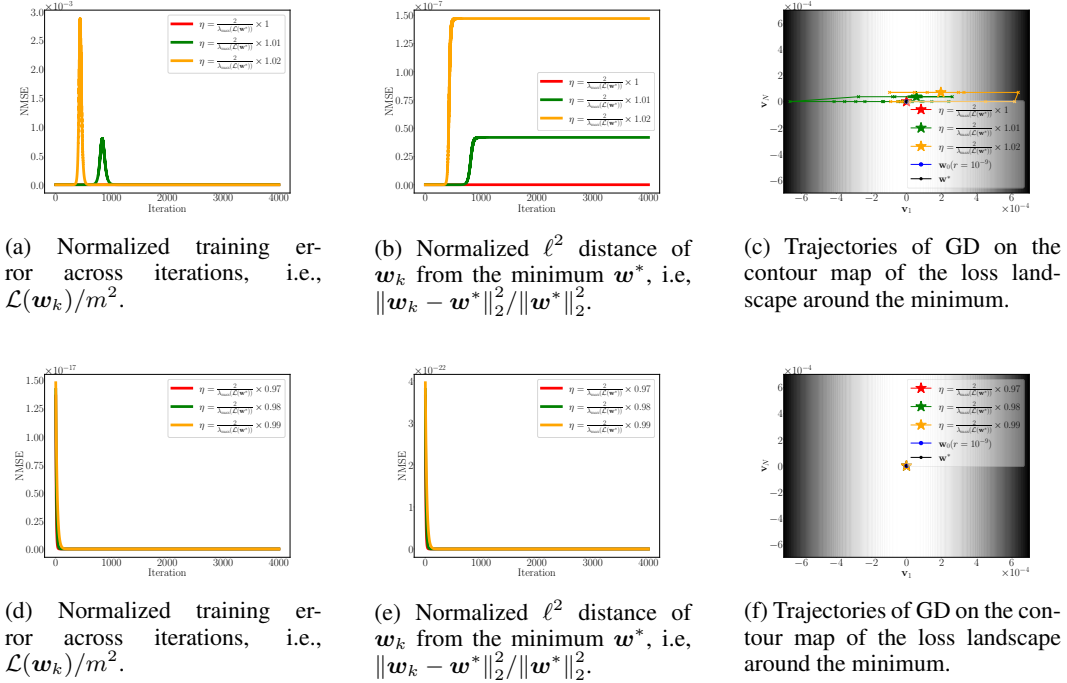


Figure 6: GD dynamics with different step sizes indicated by different colors are initialized within a radius of 10^{-9} from the minimum in the direction of the Hessian eigenvector corresponding to the largest eigenvalue, for a 20-layer overparameterized scalar factorization of a random scalar. The value of $\lambda_{\max}(\nabla^2\mathcal{L}(\mathbf{w}^*))$ is computed using the closed-form expression derived in Theorem 4.

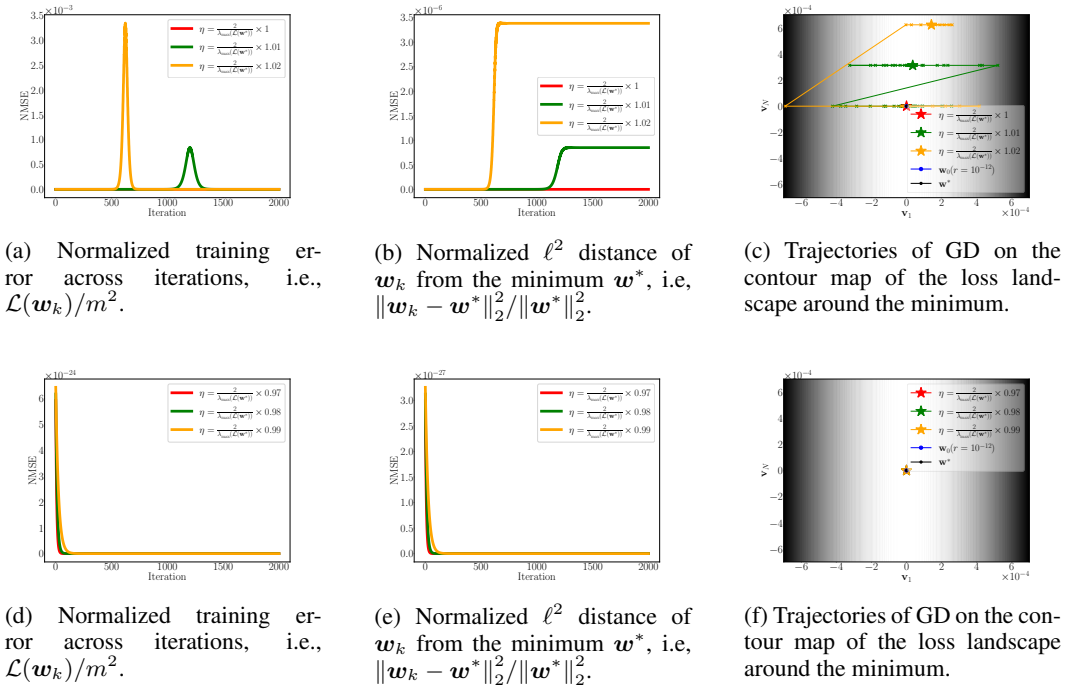


Figure 7: GD dynamics with different step sizes indicated by different colors are initialized within a radius of 10^{-12} from the minimum in the direction of the Hessian eigenvector corresponding to the largest eigenvalue, for a 5-layer overparameterized scalar factorization of a random scalar. The value of $\lambda_{\max}(\nabla^2\mathcal{L}(\mathbf{w}^*))$ is computed using the closed-form expression derived in Theorem 4.